OPEN ACCESS Freely available online

PLOS ONE

# Combining $XCO_2$ Measurements Derived from SCIAMACHY and GOSAT for Potentially Generating Global $CO_2$ Maps with High Spatiotemporal Resolution

**Tianxing Wang*, Jiancheng Shi, Yingying Jing, Tianjie Zhao, Dabin Ji, Chuan Xiong**

State Key Laboratory of Remote Sensing Science, Institute of Remote Sensing and Digital Earth, Chinese Academy of Sciences. Beijing, China

## Abstract

Global warming induced by atmospheric $CO_2$ has attracted increasing attention of researchers all over the world. Although space-based technology provides the ability to map atmospheric $CO_2$ globally, the number of valid $CO_2$ measurements is generally limited for certain instruments owing to the presence of clouds, which in turn constrain the studies of global $CO_2$ sources and sinks. Thus, it is a potentially promising work to combine the currently available $CO_2$ measurements. In this study, a strategy for fusing SCIAMACHY and GOSAT $CO_2$ measurements is proposed by fully considering the $CO_2$ global bias, averaging kernel, and spatiotemporal variations as well as the $CO_2$ retrieval errors. Based on this method, a global $CO_2$ map with certain UTC time can also be generated by employing the pattern of the $CO_2$ daily cycle reflected by Carbon Tracker (CT) data. The results reveal that relative to GOSAT, the global spatial coverage of the combined $CO_2$ map increased by 41.3% and 47.7% on a daily and monthly scale, respectively, and even higher when compared with that relative to SCIAMACHY. The findings in this paper prove the effectiveness of the combination method in supporting the generation of global full-coverage $XCO_2$ maps with higher temporal and spatial sampling by jointly using these two space-based $XCO_2$ datasets.

**Citation:** Wang T, Shi J, Jing Y, Zhao T, Ji D, et al. (2014) Combining $XCO_2$ Measurements Derived from SCIAMACHY and GOSAT for Potentially Generating Global $CO_2$ Maps with High Spatiotemporal Resolution. PLoS ONE 9(8): e105050. doi:10.1371/journal.pone.0105050

**Editor:** Juan A. Añel, University of Oxford, United Kingdom

**Received** January 3, 2014; **Accepted** July 20, 2014; **Published** August 13, 2014



**Funding:** The work described in this paper has been jointly supported by project of "Climate Change: Carbon Budget and Related Issues" (Grant nr. XDA05040402) from Chinese Academy of Sciences (CAS), the CAS/SAFEA International Partnership Program for Creative Research Teams (Grant nr. KZZD-EW-TZ-09) and National Natural Science foundation of China (Grant nr. 41301177). The funders had no role in study design, data collection and analysis, decision to publish, or preparation of the manuscript.

**Competing Interests:** The authors have declared that no competing interests exist.

* Email: wangtx@radi.ac.cn

## Introduction

In recent years, global warming caused by emission of $CO_2$ has attracted considerable attention from the public. During the past decade, although tremendous efforts have been made toward improving the understandings of the mechanism between $CO_2$ increase in the atmosphere and global warming, some uncertainties still exist in the spatiotemporal characteristics of $CO_2$ sinks/sources on regional and global scales due to the lack of high-density measurements of such variables with good accuracy [1,2]. To date, the estimates of $CO_2$ flux from inverse methods rely mainly on ground-based measurements [3,4]. Although providing highly accurate atmospheric $CO_2$ records, the traditional ground-based networks intrinsically suffer from sparse spatial coverage [2,5]. Satellite-based measurements with various spatial and temporal resolutions provide a unique opportunity to accurately map atmospheric $CO_2$ in both daytime and nighttime over large areas, thus having the potential to bridge this gap. As a result, various satellite-based platforms have been equipped in recent years for deriving the $CO_2$ concentrations.

Generally, methods for retrieving $CO_2$ from space can be grouped into two categories: (1) inferring $CO_2$ concentrations by measuring shortwave infrared (SWIR) reflected solar radiation around 1.6 and 2.0 μm with sufficient spectral resolution. This includes the Greenhouse gases Observing SATellite (GOSAT), operating since 2009 [6], the Scanning Imaging Absorption spectrometer for Atmospheric CartograpHY (SCIAMACHY), in orbit since 2002 [7], and the second Orbiting Carbon Observatory (OCO-2), which, as a rebuild of OCO [8,9], is planned to be launched in July 2014. In addition, CarbonSat will also be scheduled to be launched in 2018 (http://www.iup.uni-bremen.de/carbonsat/). These measurements have a nearly uniform sensitivity to $CO_2$ from the surface up through the middle troposphere, and thus are frequently used to derive the column-average dry air mole fraction of atmosphere $CO_2$ ($XCO_2$) during the daytime; (2) retrieving $CO_2$ concentrations by interpreting the recorded spectra of the Earth-atmosphere system in thermal infrared (TIR) bands (around 15 μm). Instruments that work in such a way include AIRS [10,11], IASI [12,13], and FTS (Band 4) of GOSAT [6]. These measurements bring the advantage that they can detect $CO_2$ during both day and night time, while the lack of sensitivity in the lower troposphere makes them inappropriate to estimate $CO_2$ near the surface where the largest signals of $CO_2$ sources and sinks occur [1]. The complementarities of these platforms allow us to combine the SWIR and TIR measurements for obtaining enhanced understanding of $CO_2$ spatiotemporal variations globally. Since $XCO_2$ is much less affected by vertical transport of $CO_2$, it is particularly useful for investigation of $CO_2$ sources and sinks using inversion modeling [14,15]. On the other hand, the spatial and temporal variations in $XCO_2$ are even

smaller than that in the surface $CO_2$; therefore, unprecedented measurement precision and accuracy are highly required for such column measurements [16–19]. SCIAMACHY (operation stopped in April 2012) and GOSAT are two typical instruments that can be used to derive $XCO_2$ from space, and a variety of retrieval algorithms have been developed for SCIAMACHY [1,20–27] and GOSAT [2,4,5,28–30] with eyes on improving $XCO_2$ retrieval accuracy to a great extent. At present, a number of $XCO_2$ products have been released. These will definitely enhance our understanding of the global carbon cycle.

Unfortunately, almost all typical instruments currently used to derive atmospheric $CO_2$ concentration are working in the infrared spectral range (less than 16 μm). Thus, except for the instrument's observation mode (for example, GOSAT observes in lattice points), the spatial coverage of the derived $CO_2$ is severely restricted by the presence of clouds. In addition, the lower signal-to-noise level over ice/snow covered surfaces and ocean for SWIR instruments (e.g., SCIAMACHY) also contributes to the $CO_2$ sparse coverage. For instance, it has been pointed out that only about 10% of GOSAT data can be used for retrieval of $XCO_2$ due to the cloud contaminations [4]. The amount of $CO_2$ measurements will be even smaller if additional screening criteria such as quality of spectral fit, aerosol loadings, etc. are further applied. Although the amount of remaining $CO_2$ measurements from certain space-based instruments may largely surpass that of ground-based sites, it is still not sufficient enough for accurately quantifying the spatiotemporal distribution of $CO_2$ over the global scale. As a result, it is greatly desired to jointly use these available $CO_2$ measurements derived from various space-based data. Recently, a novel method has been proposed for combining $CO_2$ values from seven different algorithms, and a new Level-2 $CO_2$ database (EMMA) from one algorithm is composed according to the median of monthly average of seven $CO_2$ products in each $10^\circ \times 10^\circ$ latitude/longitude grid box [31]. In fact, this method cannot increase the number of $CO_2$ observations but chooses a product with moderate oscillation among the available products. Despite the usefulness of the $XCO_2$ measurements (Level 2) in their own right, further spatiotemporal analysis for interpreting their scientific merit is essentially necessary due to the retrieval uncertainties and sparse coverage of such Level-2 observations [32]. For this point, many works have attempted to generate global full-coverage (i.e., Level 3) maps from $XCO_2$ values derived from single satellite observations using a geospatial statistics approach [32–34]. However, as reflected in these studies (for instance, Fig. 1 in the work of [33]), a compromise has to be made between the interpolated accuracy and the spatiotemporal resolution of Level-3 product because of the limited amount of Level-2 $XCO_2$ observations being used. For this point, instead of using Level-2 $XCO_2$ from a single dataset (e.g., GOSAT or OCO-2) as performed in the existing literature, we attempt to explore the potential of combining two $CO_2$ datasets (GOSAT and SCIAMACHY) in assisting in global Level-3 generation, aiming to: (1) propose a general strategy for combining (fusing) various $CO_2$ datasets with different instruments, algorithms, averaging kernels, etc.; and 2) increase the number of daily $CO_2$ points (utilized in Level-3 map interpolations) through the combination of two datasets, so that potentially improved Level-3 maps with higher accuracy and shorter time scale can be generated. The better the interpretation of the satellite-based $CO_2$ observations one can make, the higher the resolution (both temporal and spatial) of the generated global $CO_2$ maps.

## Datasets

For GOSAT, the Fourier transform spectrometer (FTS) on GOSAT is the fundamental unit to retrieve atmospheric $CO_2$ and $CH_4$. It observes sunlight reflected from the earth's surface, and light emitted from the atmosphere and the surface. It is composed of three narrow bands in the SWIR region (0.76, 1.6, and 2.0 μm) and a wide TIR band (5.5–14.3 μm) at a spectral and spatial resolution of 0.2 $cm^{-1}$ and 10.5 km, respectively [35]. Specifically, four $CO_2$ products from GOSAT have currently been released to the public: University of Leicester product [9,36], the RemoTeC product [28], NIES GOSAT product [35] and the product generated by NASA's Atmospheric $CO_2$ Observations from Space (ACOS) team (hereafter called ACOS product) [2,30]. The difference between some of the above mentioned products with various versions have been investigated in a recent study [37]. In the present paper, the ACOS product of 2009–2010 with version v2.9 has been employed.

SCIAMACHY was successfully launched on board Environmental Satellite (ENVISAT) in 2002 (unfortunately ceased in April 2012), which is a detector elements satellite spectrometer covering the spectral range 0.24–2.38 μm with a moderate spectral resolution of about 0.2–1.6 nm, and spatial resolution at nadir of 60×30 km [7]. It has eight spectral channels, with 1024 individual detector diodes for each band, observing the spectral regions 0.24–1.75 μm (band 1–6), 1.94–2.04 μm (band 7), and 2.26–2.38 μm (band 8) simultaneously in nadir and limb and solar and lunar occultation viewing geometries [22]. As mentioned in Section 1, till today, a number of $CO_2$-retrieval algorithms have been developed for SCIAMACHY. The IUP/IFE of University of Bremen has released two $XCO_2$ products, i.e., WFM-DOAS product [21,22] and the Bremen Optimal Estimation DOAS (BESD) product [1,26]. In this study, the BESD product with the versions of v02.00.08 for 2009–2010 is used.

In addition, $CO_2$ profiles of CT [38] are also collected here to allow the data mentioned above to be properly fused. CT is a NOAA data assimilation system, which provides the 3D profiles of $CO_2$ mole fractions in the atmosphere over the globe. For this study, CT data with version CT2011 is collected. This dataset provides global $CO_2$ profiles with $3^\circ \times 2^\circ$ latitude/longitude grid and 3 hours temporal resolution (a total 8 times from 01 to 22 in UTC) spanning the time period from January 2000 to December 2010. The CT dataset is used here mainly to assist in adjusting and time-shifting of the two $CO_2$ products being combined.

## Methodologies

For combining the different space-based $CO_2$ measurements, three steps are adapted in this study. First, taking the global ground measurements of $CO_2$ as reference, remove the bias of the individual $CO_2$ retrievals for ensuring the accuracy of the fused $CO_2$ product; then make some adjustment for both the ACOS and BESD products, so that they can be physically comparable and thus combined; finally fuse the ACOS and BESD $CO_2$ products considering their retrieval uncertainties, spatial scales, differences in averaging kernels and overpass times, etc.

### 3.1 Global bias corrections

Removal of any global bias of the retrieved $CO_2$ when compared with the ground *in situ* measurements is essential before performing joint use. Many researches [4,25] frequently pointed out that $CO_2$ retrievals from GOSAT are low biased with different levels due to the uncertainties in pressure, radiometric calibration, line shape model, cloud and aerosol scattering, etc.

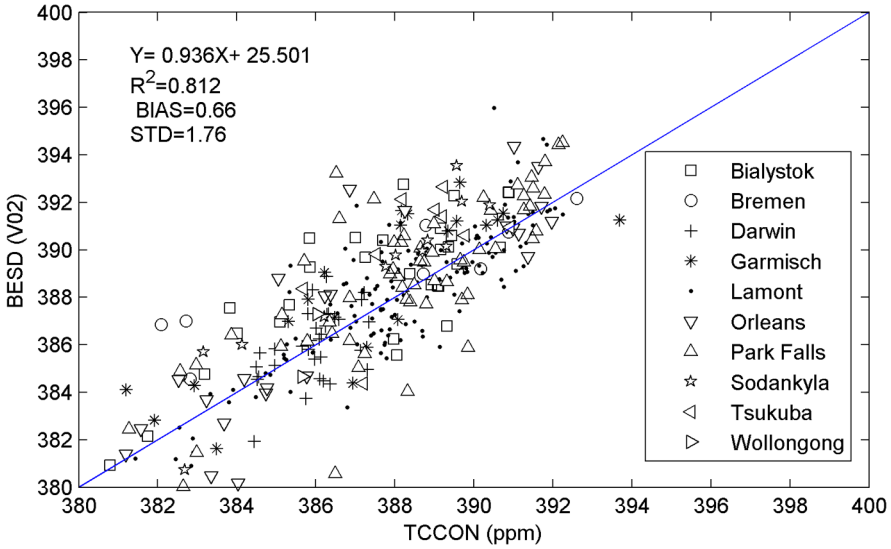


**Figure 1. Validation of the BESD products against *in situ* TCCON $CO_2$ measurements over globe for 2009–2010.**
doi:10.1371/journal.pone.0105050.g001

Fortunately, a recent study has proposed a method for evaluating systematic errors in $CO_2$ and showed that the new version of ACOS product (v2.9) has a low global bias (<0.5 ppm) [39]. Thus, there is no global bias correction for the ACOS product being conducted here, but only the ACOS retrievals that pass the filter of table B1 in the work of [38] and marked as "good" in the quality flag are used. For the BESD product, we select Total Carbon Column Observing Network (TCCON) [15] measurements for 2009–2010 as the ground truth to determine its global bias. Specifically, BESD retrievals within ±2.5° and ±2.5° latitude/longitude box centered at each TCCON site and the mean FTS value (within ±1 h time window of satellite overpass time) are

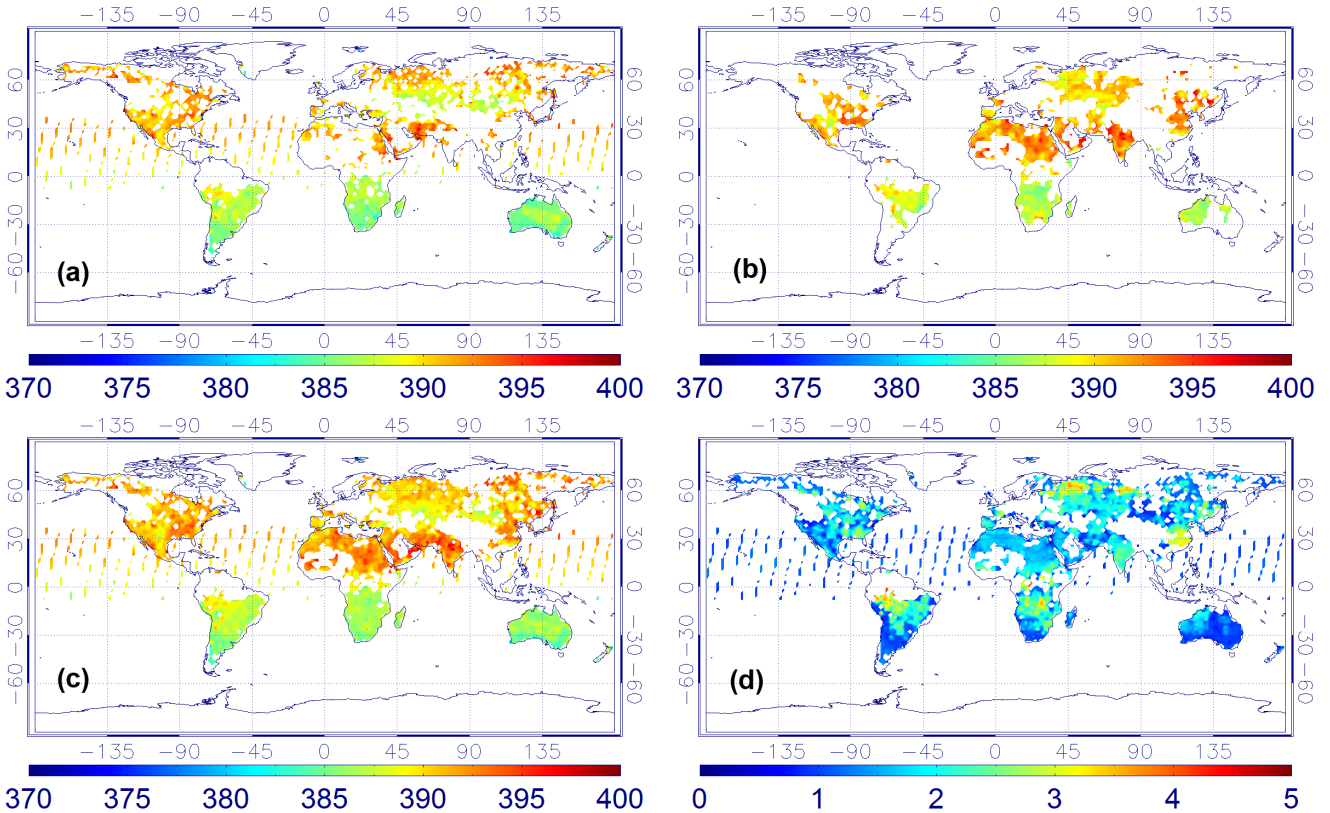


**Figure 2. $XCO_2$ monthly mean maps in May of 2010.** ((a) ACOS $XCO_2$, (b) BESD $XCO_2$, (c) combined product, and (d) $XCO_2$ uncertainties of the combined product).
doi:10.1371/journal.pone.0105050.g002

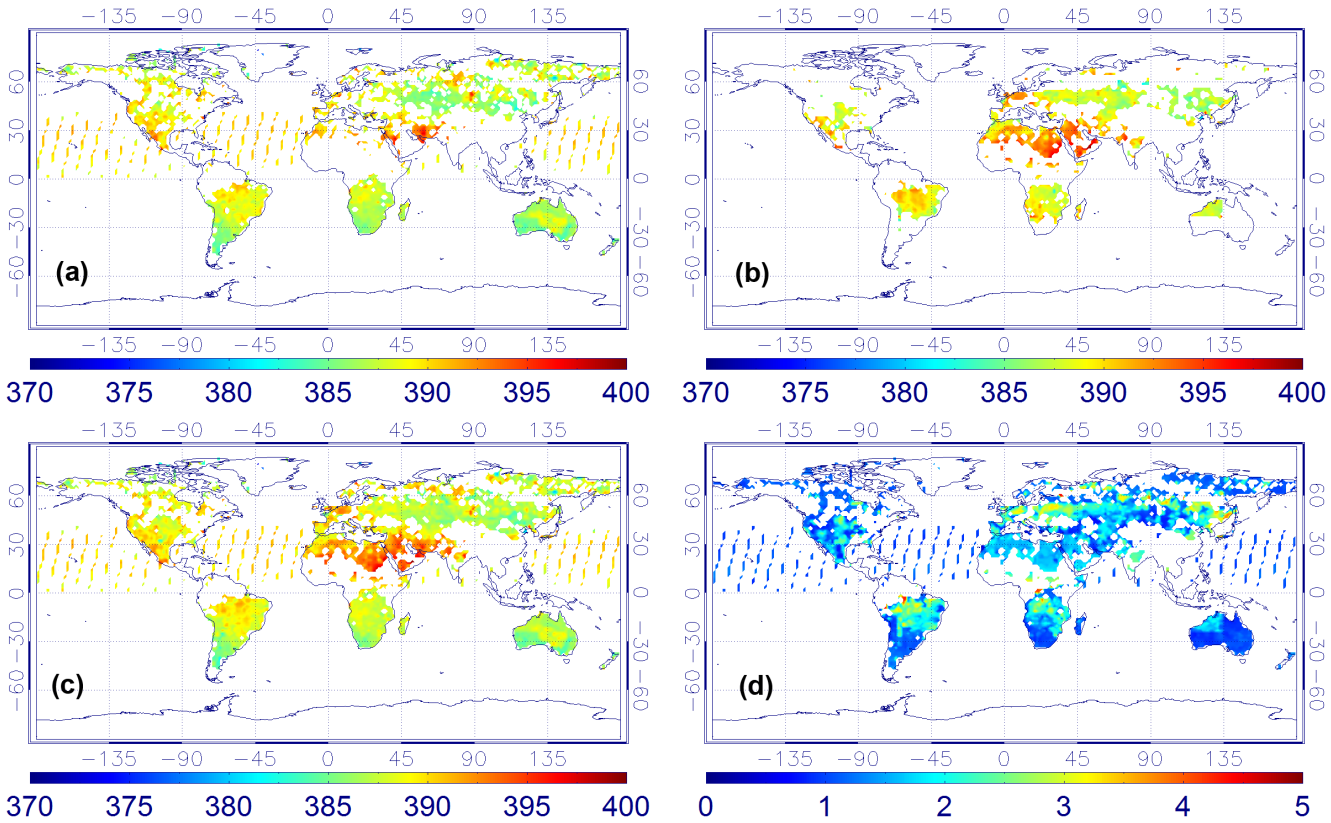


**Figure 3. $XCO_2$ monthly mean maps in June of 2010.** ((a) ACOS $XCO_2$, (b) BESD $XCO_2$, (c) combined product, and (d) $XCO_2$ uncertainties of the combined product).
doi:10.1371/journal.pone.0105050.g003

extracted and compared (totally ten TCCON sites are utilized). The coincidence criteria mentioned above ultimately yield a total of 338 pairs of $CO_2$ measurements. The comparison result is shown in Fig. 1.

### 3.2 Retrieval adjustments

As pointed out by most researchers, it is not reasonable to directly compare or use two $XCO_2$ measurements. A suitable way to do that is to take the a priori profiles and variations in averaging kernel into account during the comparison [26,40]. To tackle the a priori issue, after correcting their global biases, both BESD and ACOS products are adjusted for a common a priori profile, which we assume to be the CT profile interpolated at the middle of the two overpass times (Equation (1)). Specifically, the a priori $CO_2$ profile of both the ACOS and BESD are first interpolated or extrapolated to the level of the CT $CO_2$ profile according to their pressure layers. After interpolation, the a priori profiles for both ACOS and BESD have the same dimension as the CT profile. Here the reason we take the CT profile at the middle of the two overpass times is that the time difference for GOSAT (1:00 pm) and SCIAMACHY (10:00 am) is relative large (3 hours), if we take one satellite time as reference, the induced error would be large for the other satellite measurements considering the $CO_2$ natural diurnal variation. So a middle time between these two satellite overpass times is selected for minimizing the $CO_2$ uncertainties during the adjustment.

$$XCO_2\_adj = XCO_2\_ret + (h^T I - a)(xCT - xa) \qquad (1)$$

Here, $XCO_2\_adj$ is the adjusted $XCO_2$ for ACOS or BESD; $XCO_2\_ret$ corresponds to retrieved $XCO_2$ of ACOS or BESD; $a$ is the column-averaging kernel (row vector) of ACOS or BESD; $h$ is pressure-weighting function (column vector); $I$ is an identity matrix; $xCT$ and $xa$ (column vectors) are the common CT $CO_2$ profile and the corresponding a priori $CO_2$ profile for ACOS or BESD, respectively.

While it is not trivial to accurately consider the smoothing error without an estimate of the true atmospheric variability which is generally not readily available for most cases [39]. Fortunately, some works revealed that the smoothing error is generally small [26,39]. Consequently, for the remainder of this paper, only the adjustment in Equation (1) is applied for both the ACOS and BESD $CO_2$ products (after bias corrections).

### 3.3 Combination and time shifting

Based on the processes described above, the world is divided into a number of 0.5°×0.5°latitude/longitude grid box (totally 720×360). For each grid cell, Equation (2) is used to combine the corresponding $CO_2$ measurements within that grid.

$$XCO_2\_Fued = \sum_{i=1}^{m}\left(XCO_2\_i \times \frac{1 - Uncert\_ratio^i}{\sum_{i=1}^{m}(1 - Uncert\_ratio^i)}\right) \qquad (2)$$

where $XCO_2\_Fued$ is the combined $XCO_2$; $m$ is the total number of space-based $CO_2$ retrievals (ACOS and/or BESD) within a certain grid; $XCO_2\_i$ is the $i$th $XCO_2$ retrieval in a grid for which

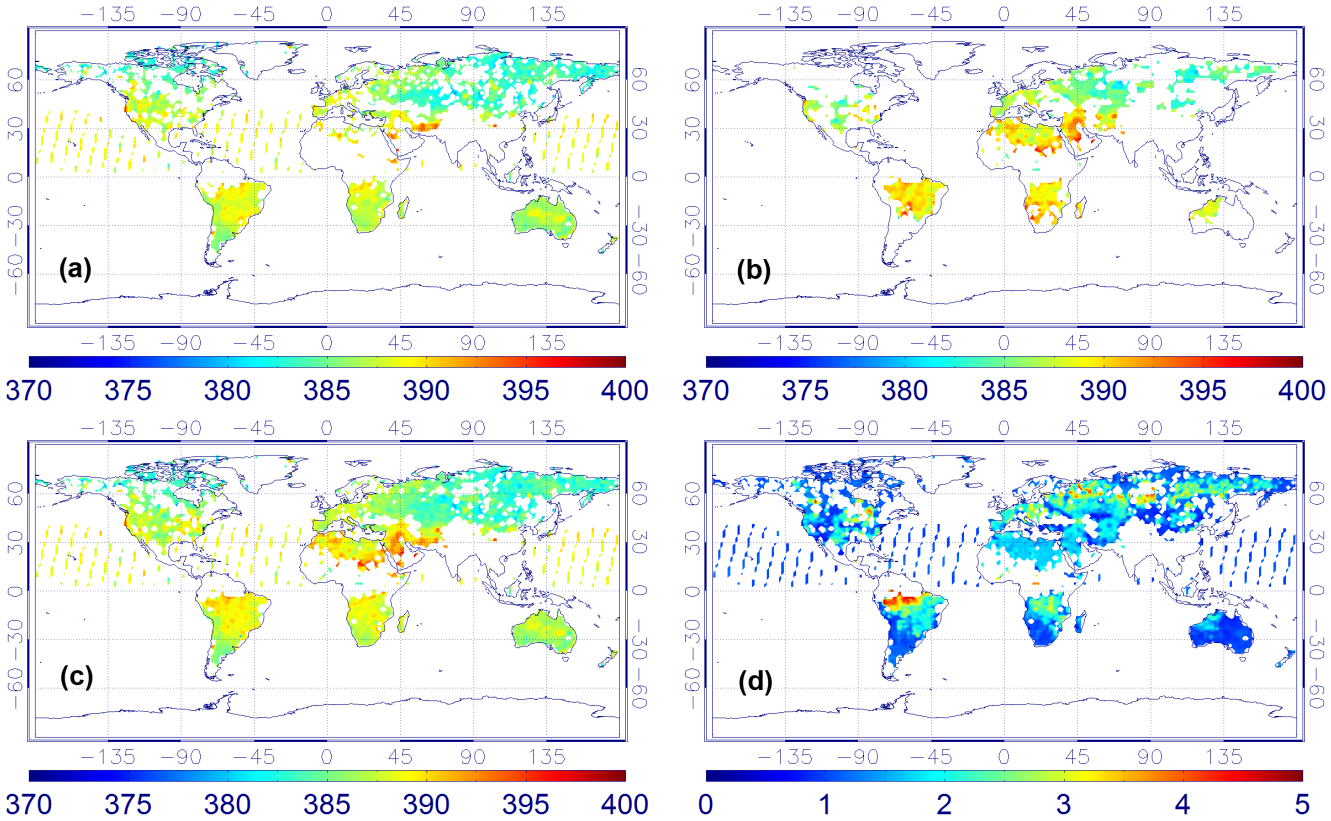


**Figure 4. $XCO_2$ monthly mean maps in July of 2010.** ((a) ACOS $XCO_2$, (b) BESD $XCO_2$, (c) combined product, and (d) $XCO_2$ uncertainties of the combined product).
doi:10.1371/journal.pone.0105050.g004

the global bias and Equation (1) are supposed to be applied; $Uncert\_ratio^i$ is the ratio of uncertainty of the $i$th $XCO_2$ retrieval to its $XCO_2$ value.

Please note that since different $CO_2$ retrievals have distinct overpass times, it is necessary to unify them to avoid uncertainties induced from the time discrepancy before fusion. To this end, a method for considering the $CO_2$ shifting along time has been developed (Equation (3)). First, designate a specific time or select one overpass time as reference, then transfer $CO_2$ measurements at various overpass times to that of the reference time by interpolating the CT $CO_2$ at temporal scale. Here, it should be pointed out that despite the $CO_2$ absolute values of CT not being accurate enough, the daily cycle pattern of atmospheric $CO_2$ it reflects is assumed to be correct.

$$XCO_2\_ref = \frac{\omega^T X\_ref^{CT}}{\omega^T X\_t^{CT}} \times XCO_2\_t \qquad (3)$$

Here, $XCO_2\_ref$ is the transformed $XCO_2$ (ACOS or BESD) at the reference time; $XCO_2\_t$ is the retrieved $XCO_2$ from ACOS or BESD at overpass time $t$; $X\_ref^{CT}$ and $X\_t^{CT}$ are $CO_2$ profiles of CT at times of reference and $t$, respectively; $\omega$ is the pressure-weighting vector (column vector).

Based on the time-shifting strategy proposed here, a global $CO_2$ map at any specific time can be theoretically produced by employing the pattern of the $CO_2$ daily cycle reflected by CT data. For instance, we can unify all $XCO_2$ retrievals being combined with various overpass times to that of UTC = 1.

## Results

Evaluation analysis showed that the global bias for the BESD product is generally small. In this study, the bias of the BESD product is corrected by subtracting 0.6 ppm from all $XCO_2$ values according to the results in Fig. 1. Although the systematic bias of the $XCO_2$ retrievals is removed, it is supposed that the error characteristics (random error) within the data are still unchanged. The bias-corrected $XCO_2$ retrievals of both ACOS and BEDS are used as fundamental data for the combination algorithm.

By applying the series of processes shown in Section 3, daily, weekly, as well as monthly maps of combined $XCO_2$ for 2009 and 2010 are generated. Here, as an example, only four maps (from May to August) of monthly mean $XCO_2$ of 2010 are shown here (Fig. 2–Fig. 5). In addition, the total $XCO_2$ uncertainties of the combined product which mainly depend on the uncertainties of the original ACOS or BESD $XCO_2$ retrievals are also illustrated.

From Fig. 2–Fig. 5, it is not difficult to observe that the combined data realize the physical complementary of the two products in terms of spatial coverage. The number of valid $CO_2$ measurements in the fused product is the union of the $CO_2$ data from both the ACOS and BESD at the same geographical location. In addition, the combined $XCO_2$ demonstrates similar spatiotemporal characteristics with that of ACOS and BESD over the globe, which implies that all processes associated with the combination do not distort the essential information of the original $XCO_2$ products (ACOS or BESD). Similar findings can also be observed in the daily mean and weekly mean $XCO_2$ maps. To quantitatively investigate the improvement of fused $XCO_2$ in spatial coverage, the fractional coverage of all three variables

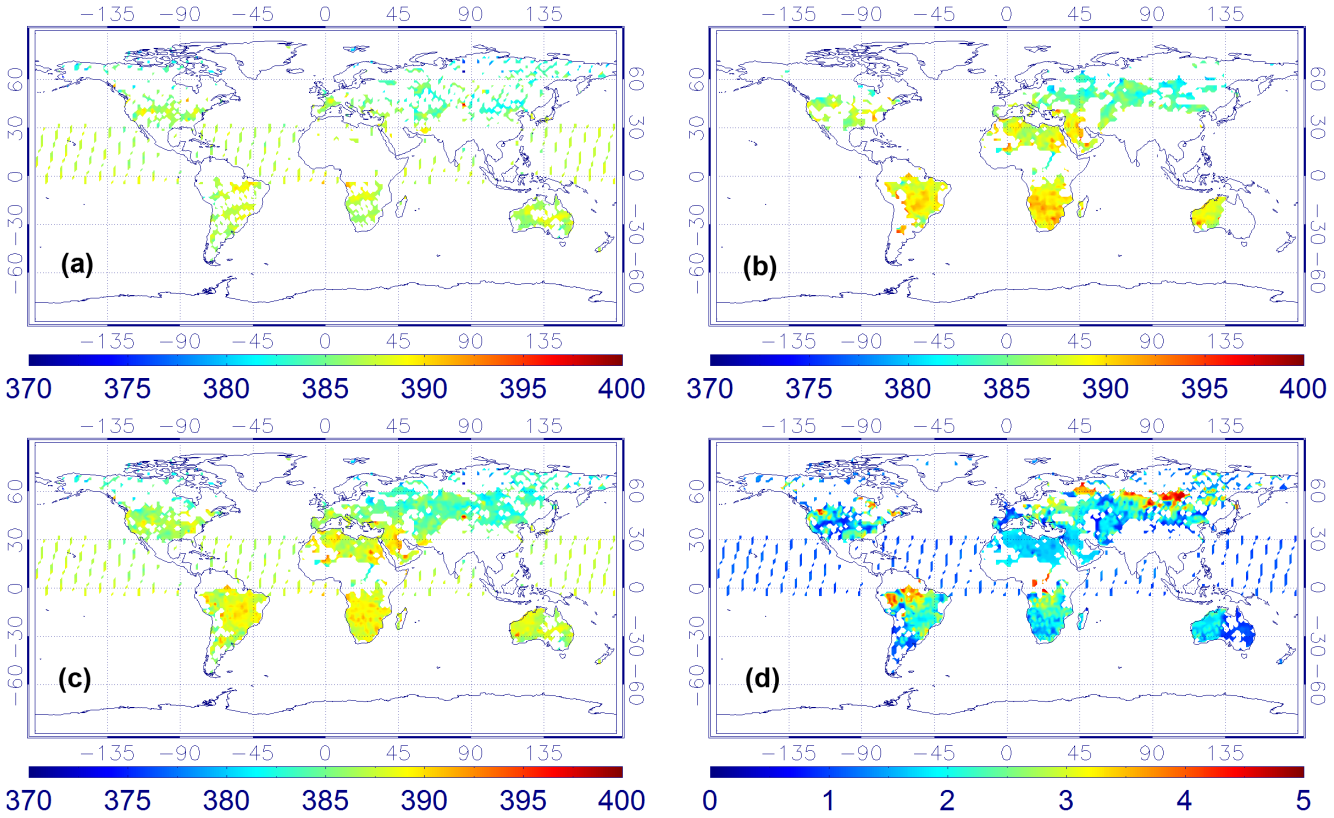


**Figure 5. $XCO_2$ monthly mean maps in August of 2010.** ((a) ACOS $XCO_2$, (b) BESD $XCO_2$, (c) combined product, and (d) $XCO_2$ uncertainties of the combined product).
doi:10.1371/journal.pone.0105050.g005

(ACOS, BESD, and combined $XCO_2$) on both daily and monthly scales is calculated (Fig. 6). From Fig. 6, it can be seen that the average global coverage of ACOS and BESD is around 0.46% and 0.21%, respectively, on a daily scale. The monthly mean coverage of such products accounts for about 5.70% and 3.75%, respectively. While spatial coverage of combined $XCO_2$ can reach up to 0.65% and 8.42% on daily and monthly scales, respectively, it accounts for increments of 41.3% and 47.7% on the daily and

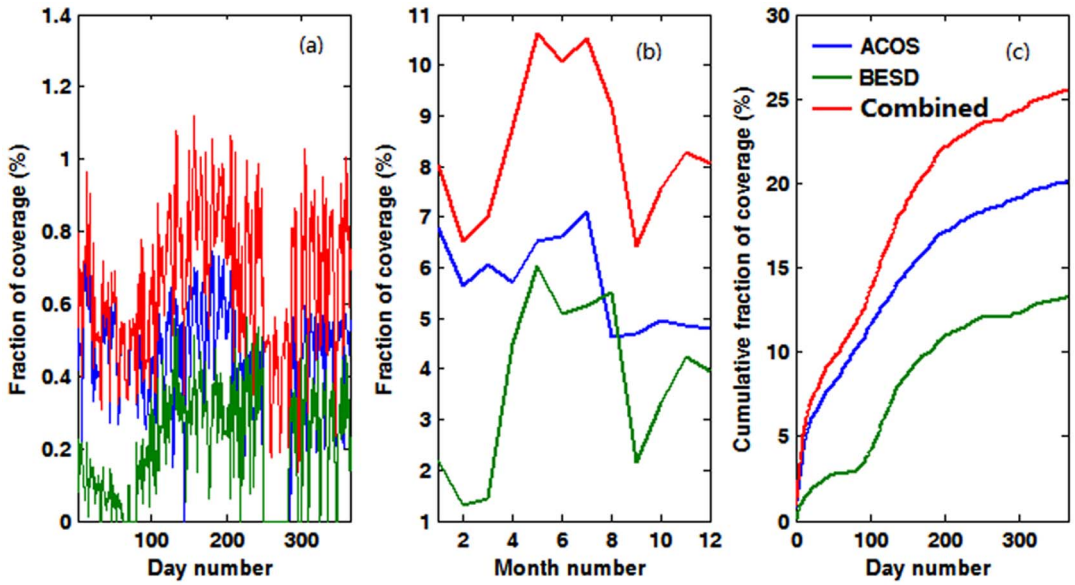


**Figure 6. $XCO_2$ fraction of coverage of ACOS, BESD, and combined products.** (a) Daily coverage. (b) Monthly coverage. (c) Cumulative coverage.
doi:10.1371/journal.pone.0105050.g006

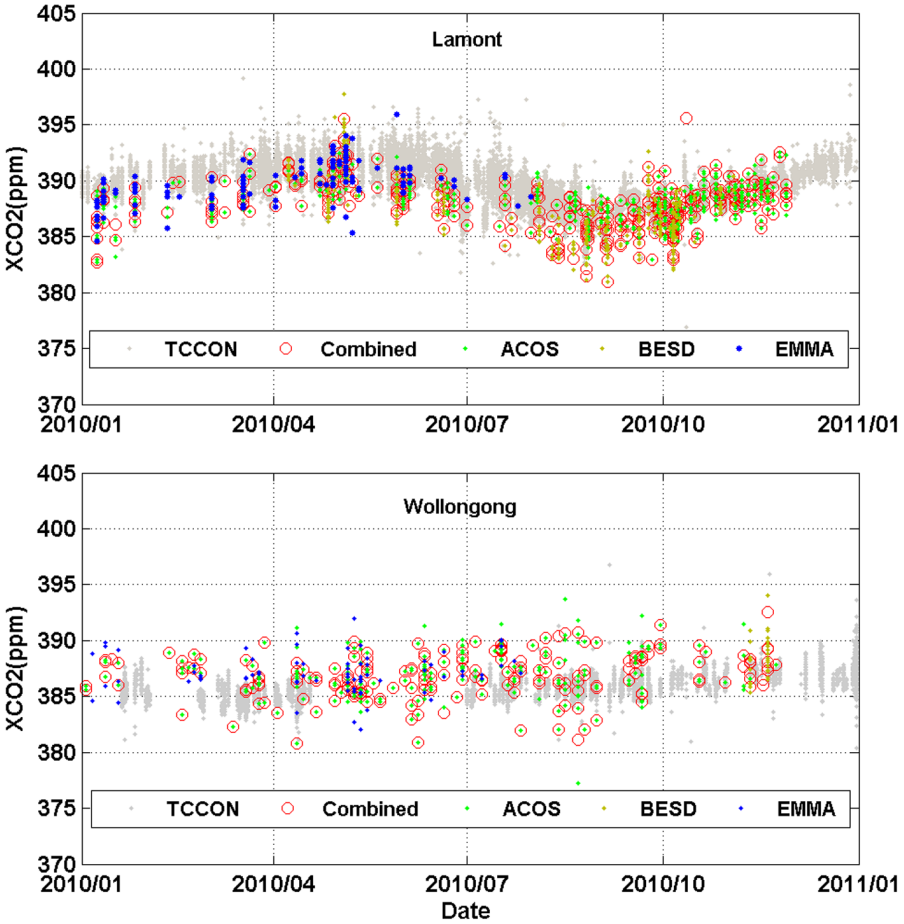


**Figure 7. Comparison of $XCO_2$ measurements from TCCON, ACOS, BESD, EMMA, and our new combination method over Wollongong and Lamont sites (distance<0.25 degree, temporal difference<1 hour).**
doi:10.1371/journal.pone.0105050.g007

monthly scales with respect to that of GOSAT and it is even higher relative to the coverage of SCIAMACHY. Likewise, the cumulative fraction of coverage of the combined $XCO_2$ has risen to 25% when compared with 20% and 13% for ACOS and BESD, respectively. The increase in the $XCO_2$ spatial coverage indicates the potential advantage of the combined $XCO_2$ observations in generating global Level-3 $XCO_2$ maps when compared with any single dataset by providing more satellite-based $XCO_2$ retrievals used for optimal interpolating.

For evaluating the performance of our combination strategy, the combined $XCO_2$ values are compared with that retrieved from ACOS and BESD as well as $XCO_2$ in the EMMA database at two TCCON sites (Fig. 7). The results reveal that the $XCO_2$ values from the combination method show generally consistent variation in time with TCCON measurements except for a small overall bias (especially for the Lamont site). On the whole, the new combined $XCO_2$ product shows good consistency with the EMMA data, and they are comparable in terms of $CO_2$ magnitude, while the combined $XCO_2$ are shown with a longer time period, which is in line with the satellite observations, and possess more data points even over the same period.

## Discussions and Conclusions

Despite the fact that space-based measurements can provide a unique opportunity to map atmospheric $CO_2$ over large areas, the number of valid $CO_2$ measurements from a single space-based instrument is generally limited for a certain day over a specific region due to the presence of clouds. In addition, although these Level-2 $XCO_2$ retrievals themselves are very important for inversion modeling of surface carbon sources/sinks, further comprehensive analysis by investigating the spatiotemporal full-coverage $XCO_2$ (Level 3) distribution is needed for interpreting their significant scientific merit [32]. While the limited satellite observations restrict the generation of Level-3 $XCO_2$ maps with high spatial and temporal resolutions when only a single satellite-based $XCO_2$ dataset is considered. This is our main motivation in this paper.

In this study, a strategy for combining SCIAMACHY and GOSAT $CO_2$ measurements has been proposed by fully accounting for the $CO_2$ global bias, differences in averaging kernels and overpass times, and the Level-2 retrieval errors of the $CO_2$ measurements being used. The results indicated that the average global coverage of both ACOS and BESD is less than 0.5% on a daily scale, and less than 6% on a monthly scale. While spatial coverage of combined $XCO_2$ can reach up to 0.65% and 8.42% on daily and monthly scales, respectively, the comparison analysis reveals that the combined $XCO_2$ product is consistent with TCCON and EMMA in both temporal variation and magnitude except for a small bias when compared with the TCCON measurements. All these findings herein prove the effectiveness of the combination method in supporting generation

global full-coverage $XCO_2$ maps with higher temporal and spatial sampling by jointly using two space-based $XCO_2$ datasets. Similar to the existing studies (e.g. [32–34]), although these combined $XCO_2$ are not intended to be used in inverse modeling studies, they deliver a key complement for such research, and can be deemed as an independent dataset for comparison with model predictions. Similar to the existing study [31], an improved fusion approach (based on multiple $XCO_2$ datasets) to create Level-2 $XCO_2$ measurements that can be directly used for inverse modeling is also attempted and will be presented in another paper.

A last point that needs to be addressed is that although we employed $CO_2$ data of GOSAT and SCIAMACHY in this study, the proposed strategies are not restricted to such data. As a general strategy, it can be refined and adapted to further combine other $XCO_2$ products, such as OCO-2, CarbonSat, etc. in the future, and even to be applied to the fusion of other trace gases, such as $O_3$, $CH_4$.

## Acknowledgments

The authors would like to thank the SCIAMACHY team at University of Bremen IUP/IFE as well as the ACOS scientific teams for providing us the $CO_2$ products. The authors also thank the anonymous reviewers for their helpful and valuable comments to improve this work.

## Author Contributions

Conceived and designed the experiments: TW JS YJ TZ DJ CX. Performed the experiments: TW JS YJ TZ DJ CX. Analyzed the data: TW JS YJ TZ DJ CX. Contributed reagents/materials/analysis tools: TW JS YJ TZ DJ CX. Wrote the paper: TW JS YJ TZ DJ CX.

## References

1. Reuter M, Bovensmann H, Buchwitz M, Burrows JP (2010) A method for improved SCIAMACHY $CO_2$ retrieval in the presence of optically thin clouds. Atmos. Meas. Tech 3: 209–232.
2. O'Dell CW, Connor B, Bösch H, O'Brien D, Frankenberg C, et al. (2012) The ACOS $CO_2$ retrieval algorithm – Part 1: Description and validation against synthetic observations. Atmos Meas Tech 5(1): 99–121.
3. Baker DF, Law RM, Gurney KR, Rayner P, Peylin P, et al (2006) TransCom 3 inversion intercomparison: Impact of transport model errors on the interannual variability of regional $CO_2$ fluxes, 1988–2003. Global Biogeochem Cy 20: GB1002, doi:10.1029/2004GB002439.
4. Morino I, Uchino O, Inoue M, Yoshida Y, Yokota T, et al. (2011) Preliminary validation of column-averaged volume mixing ratios of carbon dioxide and methane retrieved from GOSAT short-wavelength infrared spectra. Atmos Meas Tech 4: 1061–1076.
5. Butz A, Hasekamp OP, Frankenberg C, Aben I (2009) Retrievals of atmospheric $CO_2$ from simulated space-borne measurements of backscattered near-infrared sunlight: accounting for aerosol effects. Appl Opt 18: 3322–3336.
6. Kuze A, Suto H, Nakajima M, Hamazaki T (2009) Thermal and near infrared sensor for carbon observation Fourier-transform spectrometer on the Greenhouse Gases Observing Satellite for greenhouse gases monitoring, Appl Opt 35: 6716–6733.
7. Bovensmann H, Burrows JP, Buchwitz M, Frerick J, Noel S, et al (1999) SCIAMACHY –Mission objectives and measurement modes. J Atmos Sci 56: 127–150.
8. Crisp D, Atlas RM, Breon FM, Brown LR, Burrows JP, et al (2004) The Orbiting Carbon Observatory (OCO) mission. Adv Space Res 34: 700–709.
9. Boesch H, Baker D, Connor B, Crisp D, Miller C (2011) Global Characterization of $CO_2$ Column Retrievals from Shortwave-Infrared Satellite Observations of the Orbiting Carbon Observatory-2 Mission. Remote Sens 3: 270–304.
10. Aumann HH, Chahine MT, Gautier C, Goldberg MD, Kalnay E, et al. (2003) AIRS/AMSU/HSB on the Aqua Mission: Design, science objectives, data products, and processing systems. IEEE Trans Geosci Remote Sens 41: 253–264.
11. Chahine M, Barnet C, Olsen ET, Chen L, Maddy E (2005) On the determination of atmospheric minor gases by the method of vanishing partial derivatives with application to $CO_2$. Geophys Res Lett 32: L22803, doi:10.1029/2005GL024165.
12. Phulpin T, Cayla F, Chalon G, Diebel D, Schlussel P (2002) IASI on board Metop: Project status and scientific preparation. Proceedings of the 12th International TOVS Study Conference. Lorne, Vi ctoria, Australia.
13. Turquety S, Hadji-Lazaro J, Clerbaux C, Hauglustaine DA, Clough SA, et al. (2004) Operational trace gas retrieval algorithm for the Infrared Atmospheric Sounding Interferometer. J Geophys Res 109: D21301, doi:10.1029/2004JD004821.
14. Yang Z, Washenfelder RA, Keppel-Aleks G, Krakauer NY, Randerson JT, et al. (2007) New constraints on Northern Hemisphere growing season net flux. Geophys Res Lett 34: L12807. doi:10.1029/2007GL029742.
15. Wunch D, Toon GC, Blavier JFL, Washenfelder R, Notholt J, et al. (2011) The Total Carbon Column Observing Network. Philos T Roy Soc A 369: 2087–2112.
16. Rayner PJ, O'Brien DM (2011) The utility of remotely sensed $CO_2$ concentration data in surface source inversions. Geophys Res Lett 28: 175–178.
17. Houweling S, Breon FM, Aben I, Rodenbeck C, Gloor M, et al. (2004) Inverse modeling of $CO_2$ sources and sinks using satellite data: a synthetic inter-comparison of measurement techniques and their performance as a function of space and time. Atmos Chem Phys 4: 523–538.
18. Olsen SC, Randerson JT (2004) Differences between surface and column atmospheric $CO_2$ and implications for carbon cycle research. J Geophys Res 109; D02301. doi:10.1029/2003JD003968.
19. Miller CE, Crisp D, DeCola PL, Olsen SC, Randerson JT, et al. (2007) Precision requirements for space-based $XCO_2$ data. J Geophys Res 112: D10314, doi:10.1029/2006JD007659.
20. Buchwitz M, Beek R, Burrows JP, Bovensmann H, Warneke T, et al. (2005) Atmospheric methane and carbon dioxide from SCIAMACHY satellite data: initial comparison with chemistry and transport models, Atmos Chem Phys 5: 941–962.
21. Buchwitz M, Beek R, Nol S, Burrows JP, Bovensmann H, et al. (2005) Carbon monoxide, methane and carbon dioxide columns retrieved from SCIAMACHY by WFM-DOAS: year 2003 initial data set. Atmos Chem Phys 5: 3313–3329.
22. Buchwitz M, Rozanov VV, Burrows JP (2000) A near-infrared optimized DOAS method for the fast global retrieval of atmospheric $CH_4$, CO, $CO_2$, $H_2O$, and $N_2O$ total column amounts from SCIAMACHY Envisat-1 nadir radiances. J Geophys Res 105: 15231–15245, doi:10.1029/2000JD900191.
23. Houweling S, Hartmann W, Aben I, Schrijver H, Skidmore J, et al. (2005) Evidence of systematic errors in SCIAMACHY-observed $CO_2$ due to aerosols. Atmos Chem Phys 5: 3003–3013.
24. Barkley MP, Frieβ U, Monks PS (2006) Measuring atmospheric $CO_2$ from space using Full Spectral Initiation (FSI) WFM-DOAS, Atmos Chem Phys 6: 3517–3534.
25. Schneising O, Buchwitz M, Burrows JP, Bovensmann H, Reuter M, et al. (2008) Three years of greenhouse gas column-averaged dry air mole fractions retrieved from satellite – Part 1: Carbon dioxide. Atmos Chem Phys 8: 3827–3853.
26. Reuter M, Bovensmann H, Buchwitz M, Burrows JP, Connor BJ, et al. (2011) Retrieval of atmospheric $CO_2$ with enhanced accuracy and precision from SCIAMACHY: Validation with FTS measurements and com-parison with model results. J Geophys Res 116: D04301, doi:10.1029/2010JD015047.
27. Bösch H, Toon GC, Sen B, Washenfelder RA, Wennberg PO, et al. (2006) Space-based near-infrared $CO_2$ measurements: Testing the Orbiting Carbon Observatory retrieval algorithm and validation concept using SCIAMACHY observations over Park Falls, Wisconsin. J Geophys Res 111: D23302, doi:10.1029/2006JD007080.
28. Butz A, Guerlet S, Hasekamp O, Schepers D, Galli A, et al. (2011) Toward accurate $CO_2$ and $CH_4$ observations from GOSAT. Geophys Res Lett 14: L14812. DOI:10.1029/2011GL047888.
29. Yoshida Y, Ota Y, Eguchi N, Kikuchi N, Nobuta K, et al. (2011) Retrieval algorithm for $CO_2$ and $CH_4$ column abundances from short-wavelength infrared spectral observations by the Greenhouse Gases Observing Satellite. Atmos Meas Tech 4: 717–734.
30. Crisp D, Fisher B, O'Dell C, Frankenberg C, Basilio R, et al. (2012)The ACOS $CO_2$ retrieval algorithm - Part II: Global $XCO_2$ data characterization. Atmos Meas Tech 5: 687–707.
31. Reuter M, Bösch H, Bovensmann H, Bril A, Buchwitz M, et al. (2013) A joint effort to deliver satellite retrieved atmospheric $CO_2$ concentrations for surface flux inversions: the ensemble median algorithm EMMA. Atmos Chem Phys 13: 1771–1780.
32. Hammerling DM, Michalak AM, O'Dell C, Kawa SR (2012) Global $CO_2$ distributions over land from the Greenhouse Gases Observing Satellite(GOSAT). Geophys Res Lett 39: L08804, doi:10.1029/2012GL051203.
33. Hammerling DM, Michalak AM, Kawa SR (2012) Mapping of $CO_2$ at high spatiotemporal resolution using satellite observations: Global distributions from OCO-2. J Geophys Res 117: D06306, doi:10.1029/2011JD017015.
34. Zeng Z, Lei L, Hou S, Ru F, Guan X, et al. (2014) A Regional Gap-Filling Method Based on Spatiotemporal Variogram Model of $CO_2$ Columns. IEEE Trans Geosci Remote Sens 6: 3594–3603.
35. Yokota T, Yoshida Y, Eguchi N, Ota Y, Tanaka T, et al. (2009) Global Concentrations of $CO_2$ and $CH_4$ Retrieved from GOSAT: First Preliminary Results. SOLA 5: 160–163.
36. Parker R, Boesch H, Cogan A, Fraser A, Feng L, et al. (2011) Methane observations from the Greenhouse Gases Observing SATellite: Comparison to

ground-based TCCON data and model calculations. Geophys Res Lett 15: L15807, doi:10.1029/2011GL047871.
37. Wang TX, Shi JC, Jing YY, Xie YH (2013) Investigation of the consistency of atmospheric $CO_2$ retrievals from different space-based sensors: Intercomparison and spatio-temporal analysis, Chin Sci Bull, 33: 4161–4170.
38. Peters W, Jacobson AR, Sweeney C, Andrews AE, Conway TJ, et al. (2007) An atmospheric perspective on North American carbon dioxide exchange: Carbon Tracker. Proc Natl Acad Sci U.S.A. 48: 18925–18930.
39. Wunch D, Wennberg PO, Toon GC, Connor BJ, Fisher B, et al. (2011) A method for evaluating bias in global measurements of $CO_2$ total columns from space. Atmos Chem Phys 11: 12317–12337.
40. Rodgers CD (2000) Inverse Methods for Atmospheric Sounding: Theory and Practice. World Scientific Publishing Co. Ltd.193 p.